Experimental study of the effects of a six-level phase mask on a digital holographic storage system

María-P. Bernal, Geoffrey W. Burr, Hans Coufal, John A. Hoffnagle,
C. Michael Jefferson, Roger M. Macfarlane, Robert M. Shelby, and Manuel Quintanilla

We measure the $M/\#$ and the bit-error rate of a digital holographic storage system with a $4f$ optical arrangement for three configurations: recording at the Fourier plane with and without a phase mask and recording outside the Fourier plane without a phase mask. Unexpectedly, no significant change in the dynamic range was observed when a phase mask was used to record in thick crystals. However, we show that a phase mask is a key component in a $4f$ digital holographic storage system if high-fidelity holograms with optimum volumetric density are to be stored. © 1998 Optical Society of America

OCIS codes: 090.0090, 210.4810.

1. Introduction

Holographic data storage was first proposed in the early 1960's. Much effort has recently been put into its development because of the potential to provide a fast readout rate and high capacity.[1–8] These capabilities come about through the multiplexing of two-dimensional pixel arrays with a data rate of up to 1 Gbit/sec.[9] One of the most extensively used optical configurations is the Fourier transform configuration ($4f$ configuration), shown schematically in Fig. 1. It is based on recording holograms at the Fourier transform plane of the binary input-data page. This can be accomplished in practice if a spatial light modulator (SLM) is positioned at the front focal plane of a lens and the holographic recording medium at its back focal plane. The hologram is recorded by the superimposing of a collimated beam (the reference beam) and the data-bearing beam (object beam) inside the recording medium, creating a phase grating as a result of the material photosensitivity. The output of the data page is retrieved at the back focal plane of a second lens, which performs an inverse Fourier transformation of the stored hologram, and finally a detector array (CCD) transforms the optical image into an electronic signal.

Among possible recording materials, photorefractive crystals[10] have emerged as one of the candidates for holographic storage media. Some of their attractive properties include reversibility, and thus erasability, a potentially useful response time, sensitivity, and a good dynamic range.

Storage at the Fourier transform plane offers several advantages as opposed to other holographic storage configurations. The hologram size is the smallest possible at a given pixel size, focal length, and laser wavelength, which is desirable for high volumetric densities. For an image-plane geometry to offer better density, an impractically small SLM and CCD pixels would be required.[11] Another feature is the translational invariance of the Fourier transform, which facilitates holographic systems with removable media.

However, since the SLM modulates amplitude and not phase, large intensity variations occur at the Fourier transform plane. The dc components of all data pixels interfere constructively with each other at the Fourier plane, producing a high-intensity peak on the optical axis of the system. This intense peak, which carries none of the binary information of interest yet contains half the total object-beam energy, saturates the holographic recording material at that location rapidly.

Several possible solutions have been envisioned[12–16] to spread the energy more evenly within the recording medium. One solution consists of placement of the recording medium behind (or in front of) the Fourier plane of the lens system but still between the two

M.-P. Bernal, G. W. Burr, H. Coufal, J. A. Hoffnagle, C. M. Jefferson, R. M. Macfarlane, and R. M. Shelby are with IBM Almaden Research Center, 650 Harry Road, San Jose, California 95120-6099. M. Quintanilla is with the Departamento de Física Aplicada, Facultad de Ciencias, Universidad de Zaragoza, 50009 Zaragoza, Spain.

Received 25 July 1997; revised manuscript received 13 November 1997.

0003-6935/98/112094-08$15.00/0

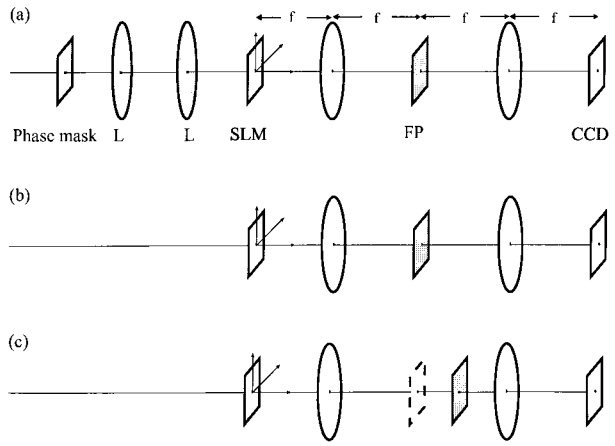

Fig. 1. Schematic of a holographic data-storage system in a 4*f* configuration when (a) recording at the Fourier transform plane (FP) using a phase mask, (b) recording at the Fourier transform plane, and (c) placing the recording medium behind the Fourier plane. The focal length of all lenses that image the SLM into the CCD is *f*. The phase mask is imaged into the data mask plane by use of a telescopic system constituted by the two lenses L.

lenses of the 4*f* system. The high-intensity peak defocuses away from the Fourier plane; so when it reaches the recording medium the maximum-intensity value has decreased, and the energy is dispersed more uniformly over a larger area.

A second proposed solution is to use a random multilevel phase mask. Burckhardt[12] was the first to introduce the concept of a two-level phase mask to overcome the problem of nonuniform intensity distributions. The idea consists of inserting a two-dimensional array of phase pixels into the 4*f* system so that it is registered pixel to pixel with the SLM. The constructive interference at the zero-frequency component is destroyed because of the random phases added to the SLM pixels. This yields a more uniform energy distribution at the Fourier transform plane and therefore a substantial reduction in the undesired saturation of the medium. Two-level phase masks have the advantage that they are simpler to manufacture than multilevel phase steps, but they do not reduce the variance of the irradiance distributions in either the hologram plane or the reconstructed image plane as effectively.[15] Recent simulations[16] indicate that one of the most optimum designs is a pseudorandom six-level phase mask. A scan of the intensity distribution at the Fourier spectrum with and without this mask can be seen in Ref. 16.

Making use of the holographic storage tester described earlier,[7] we measure and compare the three configurations mentioned above: recording in the Fourier transform plane with no phase mask or with a six-level phase mask and recording away from the Fourier transform plane. We investigate the dynamic-range performance by measuring the $M/\#$ for different object–reference intensity ratios, as well as the bit-error rate (BER) degradation (using global thresholding) of the three configurations versus the object-beam exposure.

2. Experimental Setup

The input data page was a chrome-on-glass transmission mask containing a two-dimensional array of 256×256 pixels with a 36-μm linear dimension and 100% fill factor. Random binary data were represented by means of setting approximately half the pixels to ON and the other half to OFF. Two custom lenses, each with an effective focal length of 89 mm, were used to implement the 4*f* system. The excellent optical performance of the tester permits pixel-to-pixel matching of the input data page to the detector array. A Kodak CCD with 1536×1024 pixels and 9-μm pixel spacing integrated into a Princeton Instruments Model ST138 camera was used.

For the experiments two different photorefractive media were used: a 15 mm $\times$ 15 mm $\times$ 8 mm $LiNbO_3$:Fe crystal and a 9.8 mm $\times$ 9.8 mm $\times$ 9.8 mm SBN:Ce crystal. To achieve maximum recording we used two standard geometries. The $LiNbO_3$:Fe crystal was used in 90° geometry with the *c* axis at 45° to the object and reference beams. The molar dopant concentration was 0.02%, and the absorptivity of the crystal at a wavelength of 514.5 nm was 0.8 cm^{-1}. The SBN:Ce crystal was used in transmission geometry, that is, both the object and the reference beams enter the medium through the same surface and the *c* axis parallel to this surface (X cut). The mole percent of Ce was 0.02%, and the absorptivity was 1.7 cm^{-1} at a wavelength of 514.5 nm. The object and the reference beams were ordinary polarized at all times. The reference beam was a plane wave with a 6-mm diameter. We erased the crystals before experimental runs by heating them to 200 °C for 1 h to redistribute the trapped electronic charge and erase all previous holograms.

The phase mask was a six-level phase plate[16] fabricated by means of writing with a laser on a substrate coated with photoresist. The substrate on which the phase mask was written was also antireflection coated before writing the phase mask. This phase mask was composed of a 256×256 array of linear 36-μm pixels. The mask was purely random in one direction and pseudorandom in the other [the only allowable phase difference between neighboring pixels is $\pm(\pi/3)$]. Each phase pixel was registered with the corresponding amplitude pixel in the data mask to avoid errors in the retrieval of the data page caused by diffraction effects coming from the edges of the phase pixels. When the phase mask was imaged carefully on the data-mask plane, every data pixel contained a constant random phase (from the corresponding phase pixel).

If the phase mask were to be translated along the optical axis or parallel to the data–mask plane, the field distribution at the data-mask plane would not only have multiple phase contributions but also intensity variations that distort the 1*s* and 0*s* when the image was retrieved by the CCD. To eliminate these unintended diffraction effects, we aligned and registered the two pixel arrays by imaging the phase mask onto the data-mask plane with a telescopic system of magnification equal to 1. The phase mask was

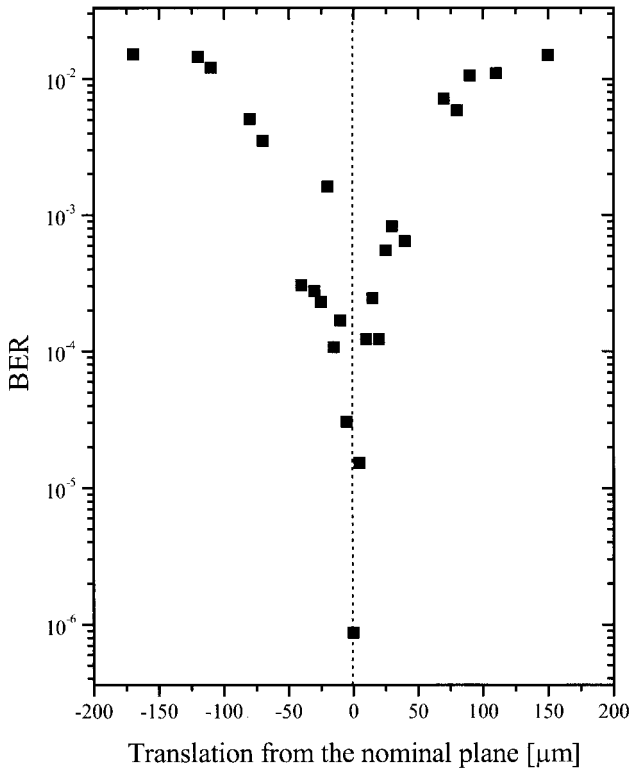

Fig. 2. BER of transmitted images as the six-level phase mask was translated along the optical axis from the nominal plane with respect to the data mask. A translation of only 100 μm produced several hundred errors in the reconstructed image.

mounted on a six-axis translation system with three orthogonal translational stages, two tilt axes, and one rotational axis. To show how critical the diffraction effects from phase pixels can be, we performed an imaging experiment in which high-quality fused silica was substituted for the crystal and the phase mask was translated along the optical axis from its nominal object plane. The results are displayed in Fig. 2, where the BER in the output image caused by diffraction is shown as the phase mask was translated along the optical axis. Defocusing the mask by only a few times its pixel size had already generated hundreds of errors in the reconstructed data image.

3. *M*/# Experiments

The $M/\#$ provides information on how a holographic data-storage system is performing in terms of dynamic range. It is a constant for a given material and recording condition.[17,18] Mathematically the $M/\#$ is defined as the constant of proportionality between the square root of the diffraction efficiency η and the number of holograms M:

$$M/\# = \sqrt{\eta}\, M. \tag{1}$$

For a photorefractive crystal the $M/\#$ can also be written in terms of the recording slope A_0/τ_r of a single hologram and the erasure-time constant τ_e:

$$M/\# = \left(\frac{A_0}{\tau_r}\right)\tau_e. \tag{2}$$

Here it is assumed that a hologram evolves during recording as

$$A_0(1 - e^{\frac{-t}{\tau_r}}) \approx \left(\frac{A_0}{\tau_r}\right)t \tag{3}$$

and decays during erasure as

$$e^{\frac{-t}{\tau_e}}, \tag{4}$$

where A_0 is the saturation strength of the hologram, τ_r is the characteristic recording time, and τ_e is the characteristic erasure time.

Phase masks change the way in which energy is distributed in the medium, modifying the object–reference-beam interaction in the recording process. This produces a different modulation depth for the low- and high-frequency components, which varies the strengths of the written diffraction gratings. On the other hand, if a phase mask is introduced into the $4f$ system the compound profile of the data-plus-phase mask at the Fourier plane tends to look like a broad slow-varying two-dimensional sinc function, creating a more uniform modulation depth throughout the entire Fourier plane.

We measured the $M/\#$ to determine if, because of the phase mask, this more equalized modulation depth in the Fourier plane enhances the dynamic range of the system. For this experiment the phase mask was aligned as closely as possible with the SLM data page. The total laser output was kept constant and equal to 70 mW. Two different experiments had to be done to obtain each $M/\#$ value, according to Eq. (2).[19] The first was a measurement of the recording slope of a single hologram A_0/τ_r, and the second a measurement of the erasure-time constant τ_e of that particular hologram. The value of A_0/τ_r was obtained directly by measurement of the diffraction efficiency η of a hologram as a function of the recording time. All the different values of A_0/τ_r were consecutively recorded by use of angular multiplexing.

The measurement of τ_e required a more elaborate experiment. During multiplexing, holograms that are recorded first are erased as subsequent holograms are written. Thus, to measure the τ_e of the target hologram, it is necessary to illuminate the recording medium with both the reference and the object beams. Exposing the material to both beams at the same time implied recording additional holograms, causing cross-talk effects that could lead us to a wrong value of τ_e. If the material were to be illuminated alternately with the object and reference beams, the experiment would take a prohibitively long time. To avoid these two problems, we performed the measurement of τ_e with the medium exposed to randomly changing object and reference beams. The reference-beam angle was varied within a 2° range, and the object-beam illumination changed as the data-mask position was moved within a range of 3 pixels, in its original plane. Measuring the diffraction efficiency η several times during the erasure process allowed us to extract the value of τ_e.

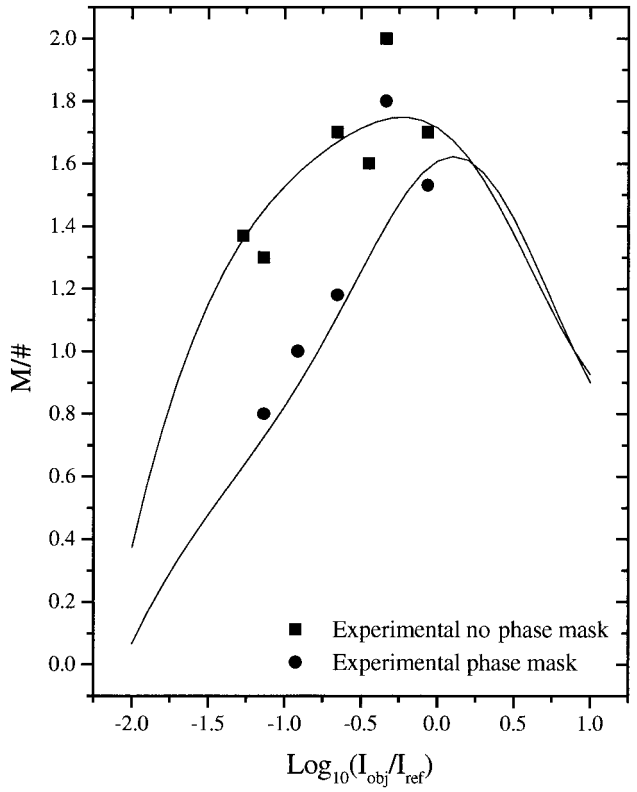

Fig. 3. $M/\#$ as a function of object–reference-beam intensity ratio in $LiNbO_3$:Fe with and without a six-level phase mask. Both measured and fitted values are displayed.

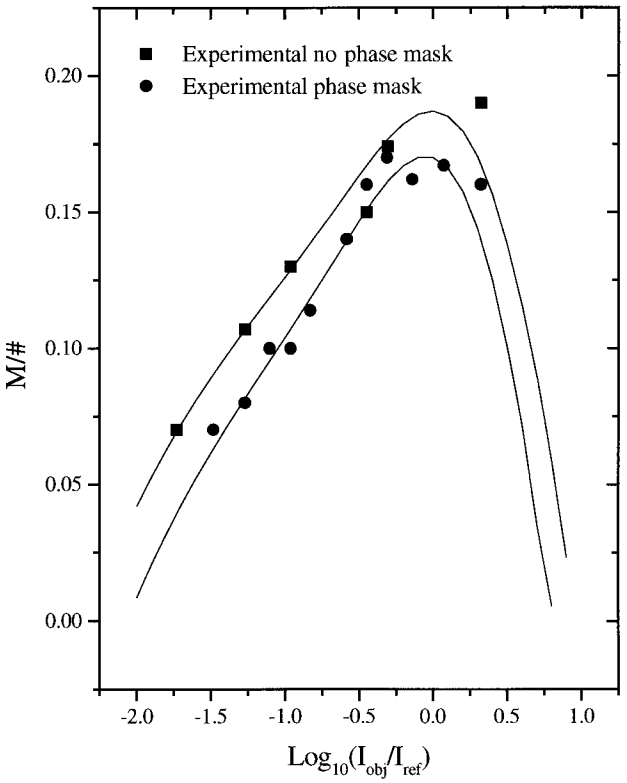

Fig. 4. $M/\#$ as the modulation depth was varied in SBN:Ce with and without a six-level phase mask. There is no significant improvement in the performance of the system when the six-level phase mask is used.

The diffraction efficiency was derived from the ON pixels at the CCD.

To obtain the object-beam intensity at the recording medium we determined the area in which the energy was distributed at the Fourier plane. We normalized the area for all the configurations analyzed in this study so that the experimental results could be compared. The area considered is within the first null of the two-dimensional Fourier transform of a single data pixel that, in our experiment, was approximately 0.0625 cm^2.

First, we studied the $LiNbO_3$:Fe crystal in the 90° geometry. A graph of the $M/\#$ as a function of the ratio between the object- and the reference-beam intensities is shown in Fig. 3. To obtain the $M/\#$ curve we fitted the erasure time constant τ_e as a function of the total intensity at the recording medium to a straight line; and the recording slope A_0/τ_r was best fitted to a third-degree polynomial (although there is, in principle, no physical reason for this). Between each erasure measurement the crystal was annealed at 200 °C for 1 h. As the object-beam power increased, the total intensity at the recording medium decreased, since losses in the object-beam path were 20 times larger than those in the reference-beam path. These extra losses are associated with beam collimations and the OFF pixels of the mask. It is clear from Fig. 3 that, although there was an optimal beam ratio, there was no noticeable improvement in the $M/\#$ when the phase mask was used.

The same experiment was performed with SBN:Ce in the transmission geometry. Figure 4 shows the $M/\#$ as a function of the ratio between object-beam and reference-beam intensities with and without the six-level phase mask. As with $LiNbO_3$:Fe, there was no major change in the $M/\#$ values for the two configurations. However, note that the $M/\#$ values for $LiNbO_3$:Fe with and without the phase mask were 1 order of magnitude larger than for SBN:Ce. One reason for this difference is the presence of an additional transport mechanism in $LiNbO_3$, namely, the bulk photovoltaic effect.

From these experimental results one can conclude that having a phase mask in the 4*f* holographic system yields no improvement to the system dynamic range despite the difference in which object-beam energy was distributed at the Fourier plane. An explanation for these unexpected results is that these holograms are stored not only at the Fourier plane but in the entire volume encompassed by the reference beam. Right at the Fourier plane, without the phase mask, the object-beam energy is stored mainly in the low-frequency components. If the reference beam contained a similar intensity, low-frequency component gratings would be strong but those developed in the rest of the plane would be very weak, resulting in low diffraction efficiency of the high-frequency components. As the dc peak propagates inside the recorded hologram, the energy is more efficiently distributed, so the strength of the gratings is

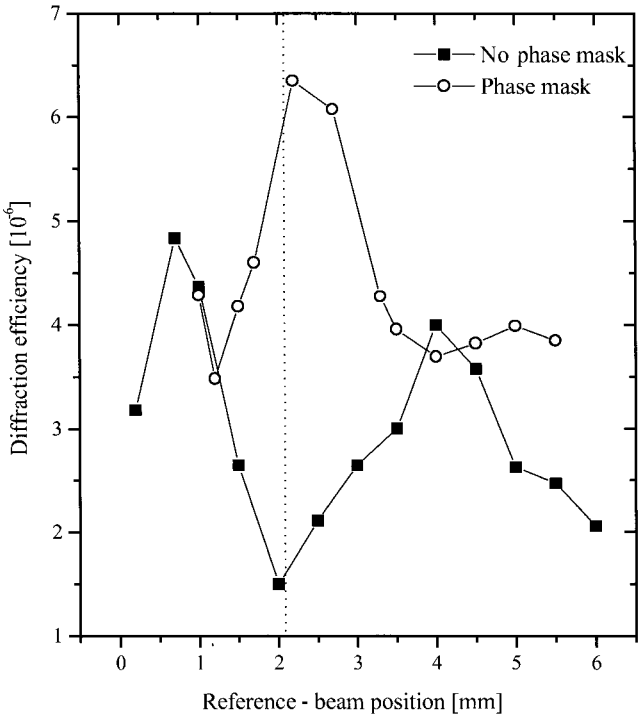

Fig. 5. Diffraction efficiency measured at different cross sections of a recorded volume hologram with and without the six-level phase mask. The origin of the x axis corresponds to the beginning of the scan. The diffraction efficiency drops dramatically at the Fourier plane when no phase mask is used, yet reaches its highest value at this plane if the phase mask is in the system.

higher and more uniform in all the frequency components. This leads to a stronger diffraction efficiency in planes away from the Fourier plane. With the phase mask the object-beam energy distribution is much more uniform, resulting in strong gratings over all the Fourier plane and throughout the volume that resulted in high diffraction efficiencies.

To show this effect we recorded a single hologram by use of a large reference beam. During readout the reference beam was masked by a 1.7 mm $\times$ 12 mm aperture to reconstruct separately thin slices of the hologram (which were parallel to the Fourier transform plane) and to study the diffraction-efficiency evolution through the different planes. This experiment was repeated under identical conditions with and without the six-level phase mask. The results are shown in Fig. 5. The object-beam intensity at the recording medium was 45.4 mW/cm^2, and the reference-beam intensity was 1.17 mW/cm^2. The recording time was 10 s. When the phase mask was not used and the recording took place at the Fourier plane, there was a plane (the Fourier plane) in which the diffraction efficiency decreased rapidly as a result of the weak gratings formed by the high-frequency components. When the phase mask was used the Fourier plane possessed the highest diffraction efficiency along the entire hologram.

We expect that, for holograms recorded in thin media and at the Fourier transform plane of the data page, the improvement in the value of $M/\#$ with a phase mask should be noticeable. The volumetric nature of the holograms when they are written in thick crystals tends to wash out this effect.

4. Bit-Error Rate Experiments

According to the unexpected $M/\#$ results, the dynamic range of a holographic system in a 4f configuration and a thick recording medium is the same with or without a phase mask. The $M/\#$, however, contains no information on the image fidelity of the hologram. We need to determine the distribution of the intensities of all data pixels in the image and measure the BER to study the image fidelity of the hologram (using histograms). Figure 6 shows histograms of two holograms recorded under the same conditions, where the $M/\#$ was reasonably large: 1.6. If there were no noise, all the 0 and 1 pixels would have the same brightness, and the histograms would have two delta functions. By fitting the tails of the 1 and 0 distributions to Gaussians, we can obtain the BER with the global-threshold technique.[7] The histogram shown in Fig. 6(a) corresponds to the hologram recorded in $LiNbO_3$:Fe by use of the six-level phase mask and has a BER of 2.8×10^{-8}. When an identical hologram was recorded without the phase mask, the histogram shown in Fig. 6(b) was such that the 1 and the 0 distributions lay on top of each other, and the error rate was close to 50%.

To measure this effect more carefully we exposed the $LiNbO_3$:Fe crystal with just the object beam, starting from a thermally erased condition. After each illumination period (0.245 J/cm^2) the transmitted image was measured with the CCD camera. This experiment was conducted for three different configurations of the 4f arrangement (see Fig. 1): (a) using the six-level phase mask and recording at the Fourier plane, (b) using no phase mask and recording at the Fourier plane, and (c) using no phase mask but with the centers of gravity of the crystal at 1 cm and also at 2 cm behind the Fourier plane of the lens system.

The results of these experiments are shown in Figure 7. Curve (a) corresponds to recording at the Fourier plane without a phase mask; curve (b) corresponds to recording at the Fourier plane without a phase mask but with the recording medium placed 1 cm behind the Fourier plane; curve (c) corresponds to using the six-level phase mask and recording at the Fourier plane; curve (d) corresponds to using no phase mask and recording with the medium 2 cm behind the Fourier plane. If one wants to store more than one hologram with a tolerable BER, recording at the Fourier plane without a phase mask must be avoided. By analyzing the initial BER for all the configurations (before any object-beam exposure), we realized that the BER is very low (10^{-15}–10^{-13}) without a phase mask in the system. Aligning the phase mask is very time consuming, and only after very careful alignment could the initial BER be reduced to values of the order of 10^{-6}. This sensitivity to alignment is mainly due to the diffraction produced by the

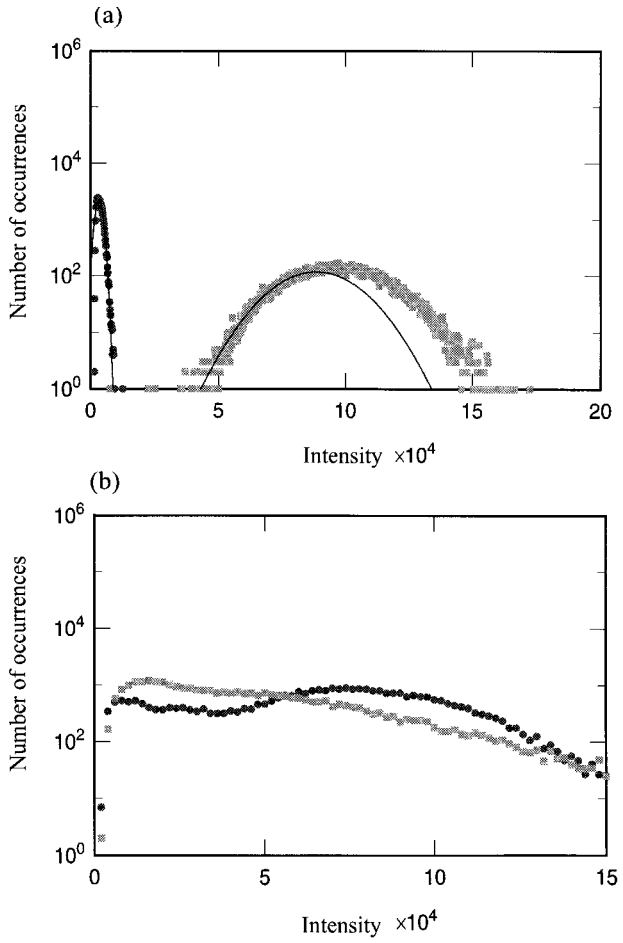

Fig. 6. Histograms corresponding to two holograms recorded at the Fourier plane in $LiNbO_3$:Fe (a) with a six-level phase mask and (b) without a phase mask. The $M/\#$ is 1.6 in both cases. With the phase mask, the BER is of the order of 10^{-8}. When the hologram is recorded at the Fourier plane without the phase mask, the material saturation is such that the output page cannot be successfully decoded.

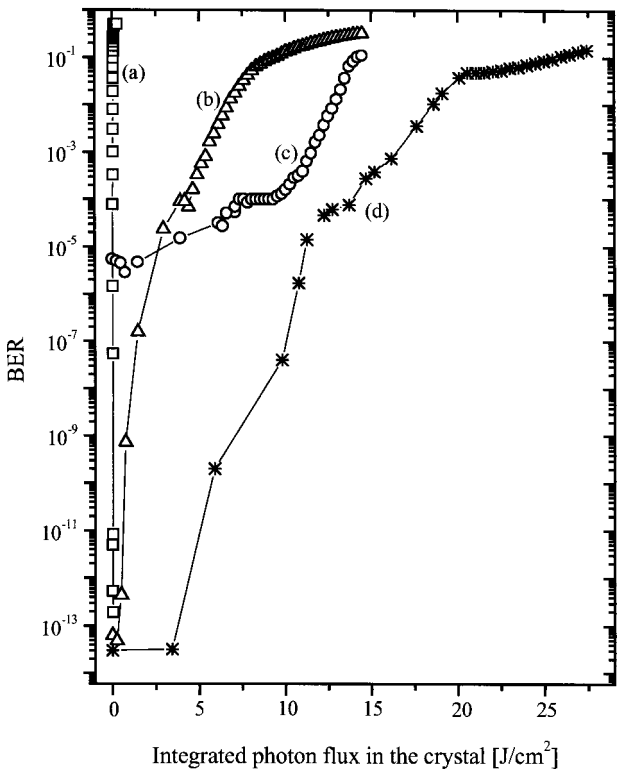

Fig. 7. BER degradation as a function of the integrated photon flux over the object-beam exposure time for four cases measured in the 4*f* configuration: (a) Recording at the Fourier plane without a phase mask. (b) Recording 1 cm away from the Fourier plane without a phase mask. (c) Recording at the Fourier plane by use of a six-level phase mask. (d) Recording 2 cm away from the Fourier plane without a phase mask.

higher phase steps in the random direction, and we believe that it could be reduced somewhat by a phase mask that is pseudorandom in both directions. In addition, a fill factor less than 100% on the amplitude SLM would help to block the phase-step transition regions between phase pixels. Additional interpixel cross-talk effects caused by the presence of a phase mask[20] contributed to increasing the initial BER.

As the integrated photon flux over exposure time increased inside the recording medium, the situation in which the material was 2 cm behind the Fourier plane was the most resistant to saturation, followed by the case in which the phase mask was used. There are two drawbacks that need to be considered when holograms are written with the medium behind the Fourier plane. First, the hologram size is larger than at the Fourier plane, therefore decreasing the volumetric density. Second, recording outside the Fourier plane can possibly make holographic storage systems with removable media more difficult. In addition, when the material is out of the Fourier plane the reference beam has to be large enough to encompass all the frequency components to reconstruct the image with the same fidelity. Since storage density is a key parameter, we believe that having a phase mask in the system is the better solution.

The same experiment was repeated without the phase mask in the object beam and with the crystal at the Fourier transform plane subjected to reference beam exposure. After an integrated photon flux in the $LiNbO_3$:Fe crystal of 8 J/cm^2, the BER increased slightly from 10^{-10} to 10^{-8}. We infer that the observed image degradation in the holograms was mainly caused by the high-intensity region of the data-bearing object beam at the Fourier plane and was unaffected by the presence of the reference beam.

To check this we investigated whether any additional saturation effects could be observed when reconstructed holograms are measured instead of transmitted images. Two different situations were analyzed: storage at the Fourier transform plane by use of the six-level phase mask and placement of the recording medium 2 cm away from the Fourier plane. Again, the recording medium was $LiNbO_3$:Fe. Holograms were written with the same object and reference power and the same exposure time as in the previous imaging experiment. A comparison between images and holograms is shown in Fig. 8 for

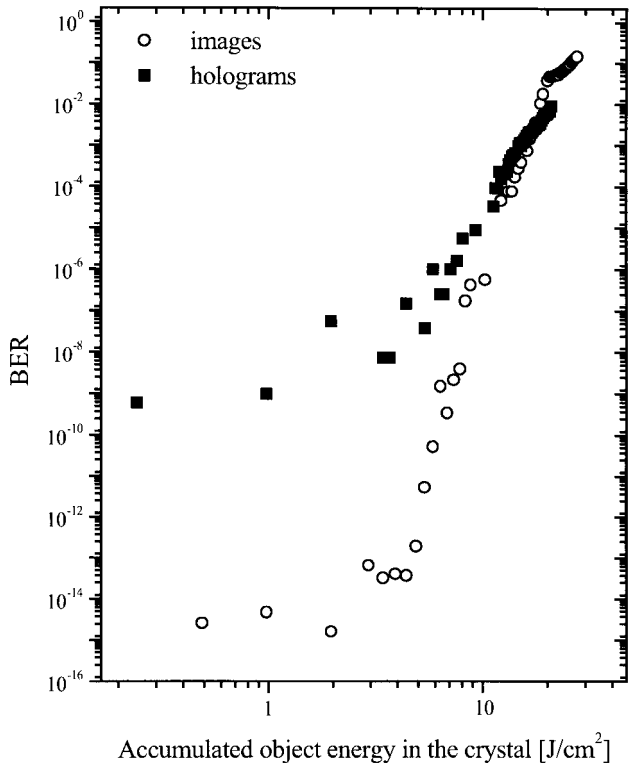

Fig. 8. Comparison of the BER degradation for images and holograms recorded with the same object-beam exposures (0.245 J/cm^2). The $LiNbO_3$:Fe crystal was placed 2 cm behind the Fourier plane.

the configuration for which the $LiNbO_3$:Fe crystal was 2 cm away from the Fourier plane. The results with the phase mask were similar. The horizontal axis corresponds to the integrated photon flux over the exposure time (object beam only). We observe that both the images and the holograms started to deteriorate after the same exposure time. When storage was 2 cm behind the Fourier plane, a BER greater than 10^{-6} occurred for an integrated photon flux of approximately 10 J/cm^2, whereas for the six-level phase mask holograms and images started to degrade at approximately 6 J/cm^2. This implies that the source of degradation came from the distortion caused by the high-intensity components of the object beam at the Fourier spectrum.

5. Conclusions

The $M/\#$ of a $4f$ digital holographic data-storage system with and without a six-level phase mask has been measured for different object–reference-beam intensity ratios at a constant total laser power. These experiments were performed in $LiNbO_3$:Fe and SBN:Ce. No major improvement in the $M/\#$ was found when a phase mask was used, despite a much more uniform energy distribution at the Fourier plane. We demonstrated that, in these thick materials, holograms are recorded not only at the Fourier plane but in the whole volume illuminated by the reference beam, and therefore the uniformity of the object-beam energy improved as the high-intensity peak propagated through the crystal, so the effects observed at the Fourier plane were averaged with those at other parts of the crystal.

The necessity of storing holograms either outside the Fourier plane or at this plane but with a phase mask became evident when BER degradation was measured as a function of the integrated photon flux over the exposure time. The use of an appropriate phase mask or storage outside the Fourier plane resulted in similar fidelity, allowing a trade-off between the complexity of alignment and the storage density.

Although a phase mask does not noticeably improve the dynamic-range performance for a thick crystal, it permits recording in the Fourier plane of the optical system, resulting in an increased storage density and removability of the media. These are both desirable features of a holographic storage technology.

This study was partially supported by the U.S. Defense Advanced Research Projects Agency under agreement MDA972-95-0004. We thank R. Kostuk and Qiang Gao from the University of Arizona for designing the six-level phase mask and Rochester Photonics Corporation for its fabrication. We also thank Robert Grygier from IBM and Glen Sincerbox from the University of Arizona for helpful discussions.

References

1. P. J. van Heerden, "Theory of optical information storage in solids," Appl. Opt. **2,** 393–400 (1963).
2. L. Hesselink and M. Bashaw, "Optical memories implemented with photorefractive media," Opt. Quantum Electron. **25,** 611–651 (1993).
3. F. Mok, "Angle-multiplexed storage of 5000 holograms in lithium niobate," Opt. Lett. **18,** 915–917 (1993).
4. J. Heanue, M. Bashaw, and L. Hesselink, "Volume holographic storage and retrieval of digital data," Science **265,** 749–752 (1994).
5. G. Sincerbox, "Holographic storage revisited," in *Current Trends in Optics*, C. Dainty, ed. (Academic, New York, 1994), pp. 195–207.
6. G. W. Burr, F. H. Mok, and D. Psaltis, "Angle and space multiplexed holographic storage using 90 degree geometry," Opt. Commun. **117,** 49–55 (1995).
7. M.-P. Bernal, H. Coufal, R. K. Grygier, J. A. Hoffnagle, C. M. Jefferson, R. M. Macfarlane, R. M. Shelby, G. T. Sincerbox, P. Wimmer, and G. Wittmann, "A precision tester for studies of holographic optical storage materials and recording physics," Appl. Opt. **35,** 2360–2373 (1996).
8. G. W. Burr, F. H. Mok, and D. Psaltis, "Storage of 10,000 holograms in $LiNbO_3$:Fe," in *Conference on Lasers and Electro-Optics*, Vol. 7 of OSA Technical Digest Series (Optical Society of America, Washington, D.C., 1994), paper CMB7, p. 9.
9. R. M. Shelby, J. A. Hoffnagle, G. W. Burr, C. M. Jefferson, M.-P. Bernal, H. Coufal, R. K. Grygier, H. Guenther, R. M. Macfarlane, and G. T. Sincerbox, "Pixel-matched holographic data storage with megabit pages," Opt. Lett. **22,** 1509–1511 (1997).
10. A. Ashkin, G. D. Boyd, J. M. Dziedzic, R. G. Smith, A. A. Ballman, J. J. Levinstein, and K. Nassau, "Optically induced refractive index inhomogeneities in $LiNbO_3$ and $LiTaO_3$," Appl. Phys. Lett. **9,** 72–74 (1966).

11. G. Barbastathis and D. Psaltis, "Comparison of the Fourier and image plane geometries for high-density holographic storage," paper presented at the OSA Annual Meeting, Rochester, N.Y., 20–24 October 1996, paper MKK7.
12. C. B. Burkhardt, "Use of a random phase mask for the recording of Fourier transform holograms of data masks," Appl. Opt. **9,** 695–700 (1969).
13. Y. Takeda, Y. Oshida, and Y. Miyamura, "Random phase shifters for Fourier transformed holograms," Appl. Opt. **11,** 818–822 (1972).
14. Y. Nakayama and M. Kato, "Diffuser with a pseudorandom phase sequence," J. Opt. Soc. Am. **69,** 1367–1372 (1979).
15. W. C. Stewart, A. H. Firester, and E. C. Fox, "Random phase data masks: fabrication tolerances and advantages of four level masks," Appl. Opt. **11,** 604–608 (1972).
16. Q. Gao and R. Kostuk, "Improvement to holographic digital data-storage systems with random and pseudorandom phase masks," Appl. Opt. **36,** 4853–4861 (1997).
17. D. Psaltis, D. Brady, and K. Wagner, "Adaptive optical networks using photorefractive crystals," Appl. Opt. **27,** 1752–1759 (1988).
18. F. H. Mok, G. W. Burr, and D. Psaltis, "System metric for holographic memory systems," Opt. Lett. **21,** 896–901 (1996).
19. G. W. Burr, "Volume holographic storage using the 90° geometry," Ph.D. dissertation (California Institute of Technology, Pasadena, Calif., 1996).
20. M.-P. Bernal, G. W. Burr, H. Coufal, R. K. Grygier, J. A. Hoffnagle, C. M. Jefferson, E. Oesterschulze, R. M. Shelby, G. T. Sincerbox, and M. Quintanilla, "Effects of multilevel phase masks on interpixel cross talk in digital holographic storage," Appl. Opt. **36,** 3107–3115 (1997).